Honors Program Theses and Research Projects

Spring 5-8-2023

Partial coalescence of CdSe/CdS Core/Shell nanocrystals

Jordyn Wray
St. Mary's University, jordynwray@gmail.com

Follow this and additional works at: https://commons.stmarytx.edu/honorstheses

Recommended Citation

Partial Coalescence of CdSe/CdS Core/Shell Nanocrystals

by
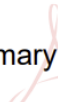
Jordyn Wray

HONORS THESIS

Presented in Partial Fulfillment of the Requirements for

Graduation from the Honors Program of

St. Mary's University

San Antonio, Texas

Approved by:

Dmitriy Khondkhon@stmary tx.edu
Digitally signed by Dmitriy Khondkhon@stmarytx.edu
Date: 2022.12.07 11:23:22 -06'00'

Dr. Dmitriy Khon

Department of Chemistry and Biochemistry

Camille A Langston
Digitally signed by Camille A Langston
Date: 2022.12.07 14:04:47 -06'00'

Dr. Camille Langston

Director, Honors Program

December 7, 2022

Abstract

Quantum dots are semiconductor nanocrystals that are a few nanometers in size that have different optical and electrical properties depending on size and shape. Some applications that quantum dots are used for, include, lasers, quantum computing, and solar cells. The goal of the research was to fuse cadmium selenide, cadmium sulfide (CdSe/CdS) core shells into dimers to increase the communication between particles in these applications. The CdSe were synthesized to 3 nm cores. Various procedures were used for CdSe/CdS synthesis, but the best performing sample contained 5 nm particles in diameter and a promising size for fusion. A metal salt for the fusion of the core shells was used to form core shell dimers. Partial coalescence to synthesize fused core shell dimers was successful with a high yield of fused particles in the solution.

Keywords: nanocrystals, CdSe/CdS, partial coalescence, high yield, fused particles

Introduction

Nanocrystals are becoming increasingly popular for inorganic research because of the cost efficiency of the material and the crystals size tunable properties. This material can be used in many applications including solar cells and QLED lights. As technology becomes more advanced, semiconductor devices are becoming more common in electronics. However, most silicon-based devices are very costly, allowing for the emergence of semiconductor nanocrystals (Kagan et al, 2016). Nanocrystals are typically 2 to 20 nm in diameter and consisting of hundreds to thousands of atoms. Some common materials of nanocrystals include CdSe, PbS, PbSe, PbTe, InP, and InAs. When used in devices, the nanocrystals must have other materials on the surface that determine the characteristics and performance of the devices (Kagan et al, 2016).

A specific application for nanocrystals is in light emitting devices. Currently, cadmium selenide cadmium sulfide (CdSe/CdS) core-shell nanocrystals are the material of choice for QD-LEDs (Shirasaki et al, 2013). CdSe emission spans the entire visible spectrum (Talapin et al, 2010). A blue shift in the emission spectrum is caused by a decrease in the quantum dot size. For nanocrystals to be added to devices, they are placed on a film. This film is comprised of two electrodes which inject a charge into a series of active layers (Supran et al, 2013). Films can also be comprised of glass, aluminum, substrates, and different types of nanocrystals (Kagan et al, 2016).

The light emitting properties of nanocrystals are explained by their tunable bandgaps (Shirasaki et al, 2013). The bandgap is defined as the energy that is needed to create an electron and hole far enough apart, so their Coulomb interaction is negligible (Brus et al, 1984). The larger the quantum dot, the smaller their band gaps become. Nanocrystals have defined energy states in the valence and conduction bands (Kagan et al, 2016). When a quantum dot is excited

by UV light, an electron in the valence band jumps to the conduction band, leaving a hole in its place. When the electron and hole recombine, a photon is emitted demonstrating light emission of the nanocrystals.

More specifically, the band gap for core shell nanocrystals is similar, but the size of the band gap is not solely determined by the size of the particle. The type of materials that the core and shell are made of determine the size of the band gap. There are three different types of band gap orientations in core shell nanocrystals: Type I, Quasi-Type II, and Type II. Type I occurs when both the electron and the hole are in the core demonstrating a similar orientation of band gap size to nanocrystals without a shell. In the case of Type II, the hole is located in the core while the electron is located in the shell. A small band gap is created in this case, dependent on the material used to synthesize the shell. Lastly, for quasi-type II the hole is located in the core and the electron can be located in either the shell or the core. This is determined by whether the core or the shell has lower energy (Toufanian et al, 2018).

As stated above, nanocrystals can be synthesized using many different metals. Cadmium is a popular precursor in the formation of nanocrystals. The shape of cadmium selenide (CdSe) nanocrystals has been well developed to form monodispersed sizes using dimethyl cadmium (Cd(CH3)2). Alternatively, using cadmium oxide (CdO) as a precursor allows for a reproducible and simple scheme that produces high quality nanocrystals (Peng et al, 2001). Nanocrystals can be synthesized with a shell of cadmium sulfide (CdS), allowing for a Type I band gap to be created. The shell helps to passivate the surface of the core, which increases its photoluminescence quantum yield and shields the core from the environment. The shell also helps to stabilize the nanocrystals in the solution and to reduce photobleaching through a large

bandgap (Eom et al, 2013). The growth of the shell is shown by a redshift in the absorbance

spectrum when analyzing the nanocrystals.

Due to the large surface to volume ratio of nanocrystals, the surface exposes different

facets of the crystals and creates dangling bonds. These bonds engage in strong chemical

bonding with ligands (Kagan et al, 2016). Ligands are organic molecules consisting of a large

carbon chain and a polar head. The surface ligands help to passivate the surface of the

nanocrystal and maintain the shape of the nanocrystal on solid films. The surface ligands help to

accelerate or inhibit the growth of the nanocrystals allowing different sizes and shapes to form.

The types of ligands commonly used for CdSe nanocrystals include amines, thiols, thiolates,

phosphine, and phosphine oxide (PO) (Schapotschnikow et al, 2009). Interactions of ligands with

the surface of the nanocrystals are described using the three types of ligands: X-, L- and Z-types.

L-type ligands are neutral and will only bind to neutral atoms. Examples of L-Type ligands

include oleylamine (OLAM), and trioctylphospine (TOP). X-type ligands are negatively charged

and bind to the positively charged metals of the nanocrystal surface. Examples of X-type ligands

include oleic acid (OA), and octadecylphosphonic acid (ODPA). Z-type ligands are neutral or

positively charged and are not commonly used during synthesis. L-type ligands cannot be

exchanged for any other ligand because the charge is not preserved, but X-type can be exchanged

for L-type ligands. This is favorable at room temperature. X- and L-type ligands bind to

cadmium while Z-type ligands bind to the selenium on the nanocrystal surface.

Coalescence is the process of combining smaller nanocrystals into a larger crystal in a

ligand-saturated solution. Traditional strategies focused on controlling the size of the nanocrystal

by controlling the precursor conversion rates. Other forms of coalescence involve nanocrystals

that are already synthesized. Nanocrystals coalesced at a low temperature cause specificity

toward the side of the nanocrystals that coalesce. Alternatively, high temperature coalescence allows random aggregation of nanocrystals to occur (Cassidy et al, 2020). Additionally, coalescence at high temperatures allows for larger, more spherical nanocrystals to form.

Fusion, partial coalescence, of nanocrystals is the process of stopping the coalescence process before large nanocrystals are formed. Fusion of CdSe/CdS core/shell nanocrystals was previously completed outside of the quantum realm on a film (Ondry et al, 2019). Another example of the fusion of core shells in solution yields size controlled fused CdSe/CdS, but through a synthesis lasting 20 hours (Cui et al, 2019). The purpose of fusing the nanocrystals is to increase the conductivity that would originally be reduced by the ligands. In optical devices, when a nanocrystal absorbs light, an exciton is formed and the electron-hole pairs. This exciton can jump between neighboring nanocrystals of the same or lower energy states (Reich et al, 2016). The fusion of the nanocrystals allows for known exciton transfer between nanocrystals. The aim of this project was to determine a reproducible procedure that results in a high yield of fused CdSe/CdS nanocrystals. This procedure is one that needs to be upscaled and consistently produce a high yield of fused nanocrystals to be utilized in industry development.

Methods

Synthesis of CdSe cores

The following procedure yields nanocrystals that are about five nanometers in diameter. The following compounds were weighed and added to a 50 mL two neck flask: 120mg of cadmium oxide (CdO), 560mg of octadecylphosphonic acid (ODPA) and 6g of trioctylphosphine oxide (TOPO). An electric stir rod was added to the flask and which was heat resistant above 300˚C. Argon in flow was inserted in the rubber stopper in one of the necks and a vacuum was

added to the other neck. The flask was degassed for 30 minutes at 150 ˚C. After 30 minutes

passed, the 25 mL flask was placed under argon and heated to 380˚C until the solution was clear.

In a smaller, 10 mL double neck flask, 116mg of selenium (Se) was weighed and added. A small

stir rod was added to the flask and was placed under argon. After enough argon passed through

the flask, 0.87 mL of trioctylphospine (TOP) was added and heated to 120˚C to dissolve. When

the solution in the 50 mL flask was clear, 3.6 mL of TOP was added and heated to 380˚C.

Immediately when 380˚C was reached, 0.87 mL of the trioctylphospine-selenium (TOP-Se)

solution was quickly added to the 50 mL flask. The solution was removed from the heat

immediately after injection and the argon flow was increased to assist with cooling. When 270˚C

was reached, the flask was placed in a water bath to cool to room temperature. At 90˚C 5mL of

toluene was added to the solution. The crystal solution was separated into 4-6 vials with 4mL of

the crystal solution and 4mL of anhydrous acetone or ethanol. The crystals were only be cleaned

once and then resubmerged in 5mL of hexane. The absorbance and emission were measured for

quantification of the crystals. The TEM machine was used to measure the diameter of the crystal

and confirm the synthesis.

Synthesis of CdSe/CdS core/shell nanocrystals

Two precursors were made for the synthesis of the core shell nanocrystals. The first

included 0.102 g of CdO, 2mL of oleic acid (OA), and 6mL of octadecene (ODE) to a 25 mL

flask with a stir rod. The solution was degassed at 120˚C for 10 minutes. After 10 minutes, the

flask was switched over to an argon flow and the temperature was increased to 220˚C and left on

the heat until clear. The second precursor included 0.34mL of octane thiol and 10mL of ODE or

30mg of sulfur (S) and 1.8 mL of TOP. If the octane thiol precursor was used it was combined at

room temperature in a tube. If the sulfur precursor was used, the sulfur was dissolved under

argon at 120˚C in a 10mL flask. For the crystal solution, 2.4mL of CdSe cores, 3mL ODE and

3mL oleylamine (OLAM) was added to a 50mL flask and degassed at 120˚C until bubbling

stopped. It was very important in this step to watch the solution to make sure it did not

overbubble into the vacuum and crystals are lost. After bubbling stopped, the temperature was

increased to 320˚C under argon. Before the temperature was increased, the precursor was set up

in an automatic injection machine. The machine was set to inject 3mL/hour. When the crystal

solution reaches 270˚C the injection was started. Injection occurred for a total of 90 minutes.

Samples were taken during the injection process to confirm the growth of the shell. After the

injection is stopped, the solution will remain on the heat for 30 extra minutes then it will be

removed and placed in a water bath when 270˚C is reached. When 120˚C was reached, 5mL of

toluene was added to the flask. After the solution reached room temperature, the crystals were

cleaned twice, first by adding 3mL of the CdSe/CdS solution and 3mL of ethanol to a tube. The

tubes were centrifuged, and the liquid was discarded. 2mL of toluene was added to the tubes to

resuspend the crystals then 2mL of ethanol was added. The tubes were centrifuged again and

then resubmerged in 5mL of hexane. The absorbance and emission were measured for the

quantification of the core/shell nanocrystals. The TEM machine was used to confirm the

synthesis of the shell and the uniformity of the solution.

<u>Fusion of CdSe/CdS nanocrystals</u>

The fusion of CdSe/CdS nanocrystals consisted of stopping the coalescence process of

the crystals. In a 25 mL two neck flask, 10mg of cadmium chloride (CdCl2), 2mL of OLAM,

and 3 units of CdSe/CdS nanocrystals were degassed at 120˚C until the bubbling stopped. After

bubbling stopped, the solution was placed under argon and the temperature was increased to

260˚C. Samples were taken during the fusion process to confirm the red shift representing the

fusion. If the emission spectrum showed the crystals were over coalescing through a widening of the peak, they were removed from the heat immediately. The emission spectrum and TEM machine were used to confirm the synthesis of the fused crystals.

Results and Discussion

A high yield of fused CdSe/CdS nanocrystals with a thiol ligand were synthesized using one procedure. The successful synthesis began with a uniform sample of CdSe cores that remained in solutions. Cores with a diameter of 3nm proved to be the most effective (figure 1D). If the cores were smaller, the shell could be grown too thick affecting the semiconductor properties of the crystals. In contrast a core that is too large would produce a shell that is too thin, and fusion coalescence would likely occur between the cores instead of stopping at the shell. In the fusion process, ligands play a vital role in the rate and effectiveness of fusion. Multiple methods were used for the synthesis of the CdSe cores, but the procedure that produced the most uniform sample utilized ODPA only instead of using steric acid (Liu et al, 2010).
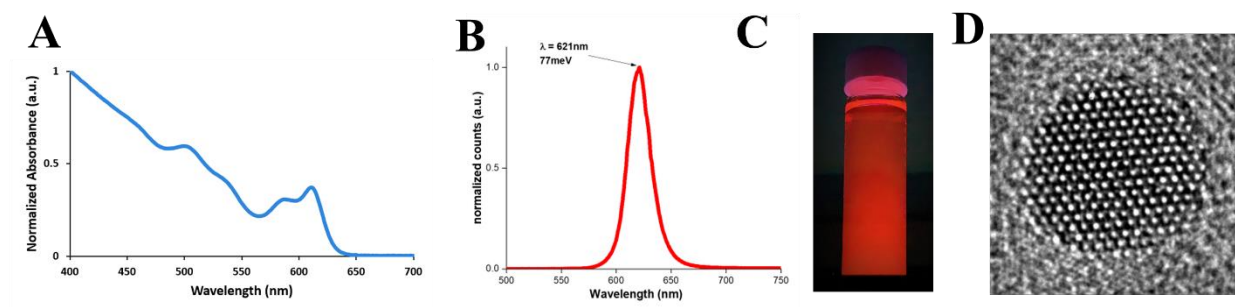
Figure 1. Confirmation of synthesis of CdSe nanocrystals. (A) Absorbance spectrum of synthesized nanocrystals with a wavelength of 610nm. (B) Emission spectrum of synthesized CdSe with wavelength of 621nm and a line width of 77meV. (C) Excited sample of CdSe

nanocrystals under UV to indicate successful synthesis of crystals. (D) TEM image of CdSe nanocrystals with all atoms shows to help confirm the size of the individual nanocrystals to 3nm.

Initially, fusion was attempted with CdSe/CdS core shell nanocrystals that were passivated by TOP-S. The synthesis of the CdSe/CdS nanocrystals were confirmed with the redshift in the absorbance and emission graphs (Figure 2A and B). As the absorbance and the emission of the crystals redshift, the size increases from 3nm to about 5nm (Figure 2B). Multiple fusion trials were attempted with these core shell crystals, all resulting in unsuccessful fusion (Figure 3C). The unsuccessful fusion was confirmed by both the TEM image and the emission spectrum. A second population was present in the sample shown by the bump at 630nm in the emission graph (figure 3A). During the attempted fusion, the core shell nanocrystals fully coalesced to form nonuniform crystals. This unsuccessful fusion could be due to the bulky nature of the ligand. During the fusion process, if the ligand cannot completely dissociate from the crystal surface, then fusion cannot occur because the ligands block the collision of the crystals.
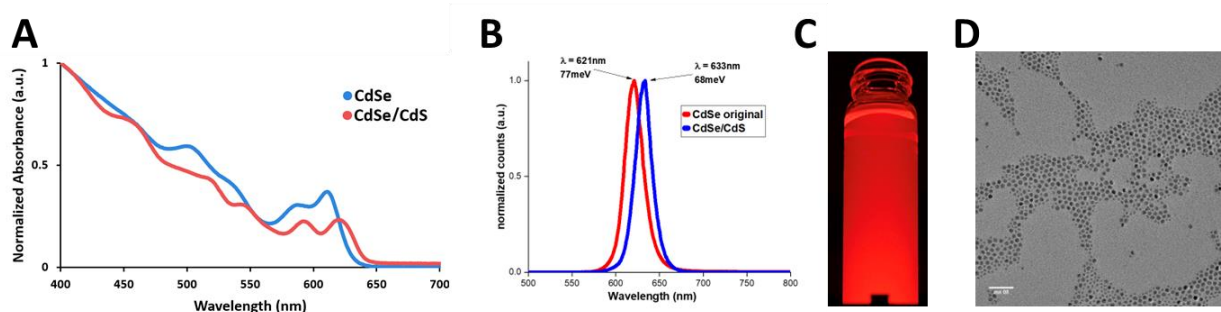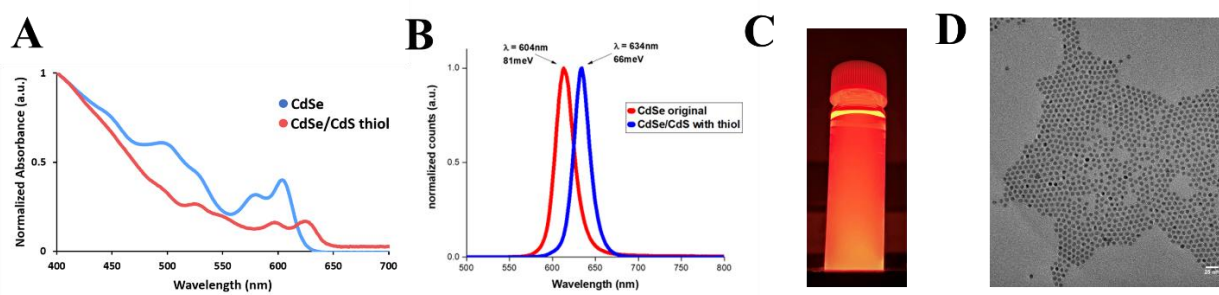

Figure 2. Conformation of synthesis of CdSe/CdS core/shell nanocrystals with TOP-S: (A) Absorbance spectrum of synthesis of CdSe/CdS core shells compared to CdSe cores. The CdSe cores were measured at 610 nm and the CdSe/CdS core shells were measured at 630 nm. (B) Emission spectrum of CdSe/CdS core shells compared to the CdSe cores. The wavelength

redshifted from 621 nm to 633 nm and the width of the line decreased from 77meV to 68meV.

(C) Excited sample of synthesized core shell nanocrystals. (D) TEM image of synthesized

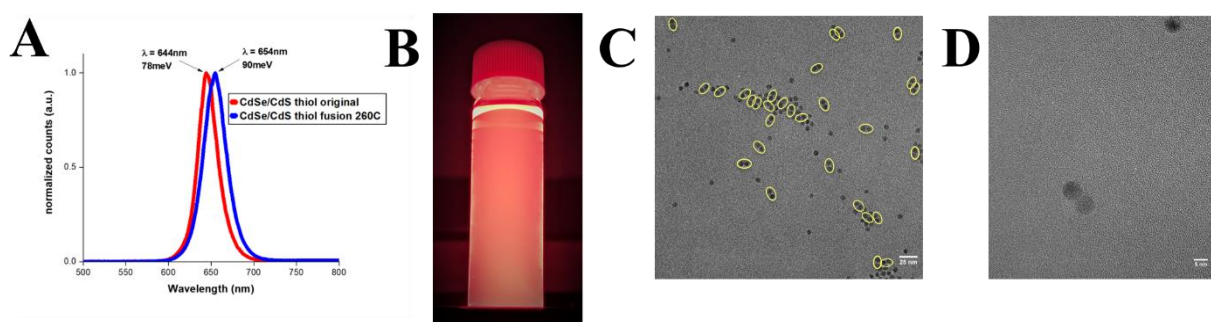CdSe/CdS nanocrystals, size of particle is 5nm.
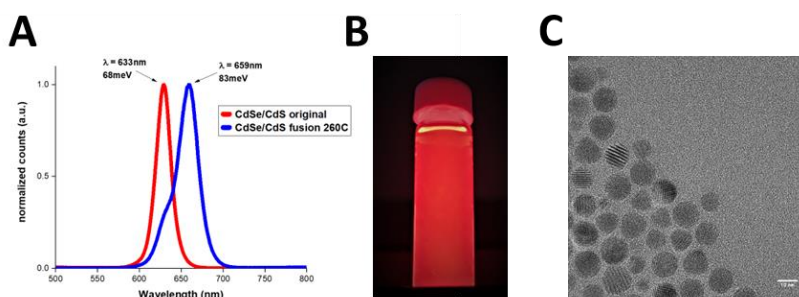
Figure 3. Confirmation of synthesis of fused CdSe/CdS TOP-S nanocrystals. (A) Synthesis

of fused CdSe/CdS core shells was completed at 260˚C. A redshift in the wavelength was

observed with the final sample at 659nm and the line width increased to 83meV. A small bump

is seen in the graph at about 630nm resulting in a possible second population forming. (B)

Excited sample of fused core shell nanocrystals after fusion. (C) TEM image of fused CdSe/CdS

core shell nanocrystals.

Figure 4. Confirmation of synthesis of CdSe/CdS core/shell nanocrystals with thiol:

(A) Absorbance spectra comparison of original CdSe to synthesis of CdSe/CdS. Wavelength has

a redshift from 610nm to 640nm. (B) Emission spectra comparison indicating a redshift in the

wavelength from 604nm to 634nm. The line width also narrowed from 81 meV to 66 meV. (C)

Excited sample of synthesized core shell nanocrystals. (D) TEM image of the synthesized

CdSe/CdS nanocrystals, size of particle is 5nm.

Synthesis with a different ligand proved to be more successful. CdSe/CdS core shell

nanocrystals were then synthesized with ODE and octane thiol. This ligand contains a single

carbon chain reducing the bulky nature of the surface ligand. The same trend was observed with

the synthesis of the core shells through the redshift of the absorbance and emission graphs

(figure 4A and B). There was a larger redshift in the synthesis of these samples which indicates a

thicker shell formed which could inhibit the communication between the particles after fusion.

Fusion was performed with these particles which resulted in a high yield sample (figure 5C). The

fusion of particles resulted in a small redshift in the emission spectrum of only 10nm (figure 5A).

A small shift was expected due to the particles only merging at the shells with the original cores

remaining intact. The TEM image confirmed the partial coalescence of the nanocrystals and a

possible successful procedure for fusion (figure 5D).

Figure 5: Confirmation of synthesis of fused CdSe/CdS thiol nanocrystals. (A) Emission

spectra comparison between synthesized CdSe/CdS nanocrystals and fused core shell particles.

This is indicated by the redshift in the wavelength from 644nm to 654nm, also the line width

broadens from 78meV to 90meV. (B) Excited sample of fused particles after fusion. (C) TEM image of successfully fused particles with a high yield sample. (D) Zoomed in TEM image of one fused dimer.

Conclusion

The study has shown the successful synthesis of fused CdSe/CdS nanocrystals using ODPA for the synthesis of the cores, and ODE and octane thiol for the synthesis of the CdS shell. The efficiency of the synthesized fused particles in applications has not been determined before my involvement in the project ended. Only one successful fusion trial was completed rendering the reproducibility of the procedure unknown. In order to determine the reproducibility, synthesis will have to be performed successful again with the same size crystals and synthesis with different sized crystals will have to be completed with a high yield of fused particles. Another aim for continued research is to fuse CdSe/CdS core shells onto a CdS rod to potentially enhance the optical properties of the crystals.

References

Brus, L. E. (1984). Electron–electron and electron-hole interactions in small semiconductor

crystallites: The size dependence of the lowest excited electronic state. *The Journal of

Chemical Physics*, *80*(9), 4403–4409. https://doi.org/10.1063/1.447218

Cassidy, J., Ellison, C., Bettinger, J., Yang, M., Moroz, P., & Zamkov, M. (2020). Enabling

Narrow Emission Line Widths in Colloidal Nanocrystals through Coalescence Growth.

Chemistry of Materials, *32*(17), 7524–7534.

https://doi.org/10.1021/acs.chemmater.0c02874

Cui, J., Panfil, Y. E., Koley, S., Shamalia, D., Waiskopf, N., Remennik, S., Popov, I., Oded, M.,

& Banin, U. (2019). Colloidal quantum dot molecules manifesting quantum coupling at

room temperature. *Nature Communications*, *10*(1), 5401. https://doi.org/10.1038/s41467-

019-13349-1

Eom, N. S. A., Kim, T.-S., Choa, Y.-H., Kim, W.-B., & Kim, B. S. (2013). Core-size-dependent

properties of CdSe/CdS core/shell QDs. *Materials Letters*, *99*, 14–17.

https://doi.org/10.1016/j.matlet.2013.02.065

Kagan, C. R., Lifshitz, E., Sargent, E. H., & Talapin, D. V. (2016). Building devices from

colloidal quantum dots. *Science*, *353*(6302), aac5523.

https://doi.org/10.1126/science.aac5523

Liu, X., Jiang, Y., Wang, C., Li, S., & Chen, Y. (2010, November 2). *White-light-emitting CdSe

quantum dots with ... - wiley online library*. Advanced Materials Interfaces. Retrieved

November 21, 2022, from

https://onlinelibrary.wiley.com/doi/full/10.1002/pssa.201026123

Ondry, J. C., Philbin, J. P., Lostica, M., Rabani, E., & Alivisatos, A. P. (2019). Resilient

Pathways to Atomic Attachment of Quantum Dot Dimers and Artificial Solids from

Faceted CdSe Quantum Dot Building Blocks. *ACS Nano*, *13*(11), 12322–12344.

https://doi.org/10.1021/acsnano.9b03052

Peng, Z. A., & Peng, X. (2001). Formation of High-Quality CdTe, CdSe, and CdS Nanocrystals

Using CdO as Precursor. *Journal of the American Chemical Society*, *123*(1), 183–184.

https://doi.org/10.1021/ja003633m

Reich, K. V., & Shklovskii, B. I. (2016). Exciton Transfer in Array of Epitaxially Connected

Nanocrystals. *ACS Nano*, *10*(11), 10267–10274. https://doi.org/10.1021/acsnano.6b05846

Schapotschnikow, P., Hommersom, B., & Vlugt, T. J. H. (2009). Adsorption and Binding of

Ligands to CdSe Nanocrystals. *The Journal of Physical Chemistry C*, *113*(29), 12690–

12698. https://doi.org/10.1021/jp903291d

Shirasaki, Y., Supran, G. J., Bawendi, M. G., & Bulović, V. (2013). Emergence of colloidal

quantum-dot light-emitting technologies. *Nature Photonics*, *7*(1), 13–23.

https://doi.org/10.1038/nphoton.2012.328

Supran, G. J., Shirasaki, Y., Song, K. W., Caruge, J.-M., Kazlas, P. T., Coe-Sullivan, S.,

Andrew, T. L., Bawendi, M. G., & Bulović, V. (2013). QLEDs for displays and solid-

state lighting. *MRS Bulletin*, *38*(9), 703–711. https://doi.org/10.1557/mrs.2013.181

Talapin, D. V., Lee, J.-S., Kovalenko, M. V., & Shevchenko, E. V. (2010). Prospects of

Colloidal Nanocrystals for Electronic and Optoelectronic Applications. *Chemical

Reviews*, *110*(1), 389–458. https://doi.org/10.1021/cr900137k

Toufanian, R., Piryatinski, A., Mahler, A. H., Iyer, R., Hollingsworth, J. A., & Dennis, A. M.

(2018). Bandgap Engineering of Indium Phosphide-Based Core/Shell Heterostructures

Through Shell Composition and Thickness. *Frontiers in Chemistry*, *6*, 567.

https://doi.org/10.3389/fchem.2018.00567